

---

# Transferable Deep Clustering Model

---

**Zheng Zhang**

Department of Computer Science  
Emory University  
Atlanta, GA 30322, USA  
zheng.zhang@emory.edu

**Liang Zhao**

Department of Computer Science  
Emory University  
Atlanta, GA 30322, USA  
liang.zhao@emory.edu

## Abstract

Deep learning has shown remarkable success in the field of clustering recently. However, how to transfer a trained clustering model on a source domain to a target domain by leveraging the acquired knowledge to guide the clustering process remains challenging. Existing deep clustering methods often lack generalizability to new domains because they typically learn a group of fixed cluster centroids, which may not be optimal for the new domain distributions. In this paper, we propose a novel transferable deep clustering model that can automatically adapt the cluster centroids according to the distribution of data samples. Rather than learning a fixed set of centroids, our approach introduces a novel attention-based module that can adapt the centroids by measuring their relationship with samples. In addition, we theoretically show that our model is strictly more powerful than some classical clustering algorithms such as  $k$ -means or Gaussian Mixture Model (GMM). Experimental results on both synthetic and real-world datasets demonstrate the effectiveness and efficiency of our proposed transfer learning framework, which significantly improves the performance on target domain and reduces the computational cost.

## 1 Introduction

Clustering is one of the most fundamental tasks in the field of data mining and machine learning that aims at uncovering the inherent patterns and structures in data, providing valuable insights in diverse applications. In recent years, deep clustering models [20, 40, 25] have emerged as a major trend in clustering techniques for complex data due to their superior feature extraction capabilities compared to traditional shallow methods. Generally, a feature extracting encoder such as deep neural networks is first applied to map the input data to an embedding space, then traditional clustering techniques such as  $k$ -means are applied to the embeddings to facilitate the downstream clustering tasks [10, 28]. There are also several recent works [33, 35, 37, 36, 15, 39] that integrate the feature learning process and clustering into an end-to-end framework, which yield high performance for large-scale datasets.

While existing deep approaches have achieved notable success on clustering, they primarily focus on training a model to obtain optimal clustering performance on the data from a given domain. When data from a new domain is present, an interesting question is can we leverage the acquired knowledge from the learned model on trained domains to guide the clustering process in new domains. Unfortunately, existing deep clustering models can be hardly transferred from one domain to another. This limitation arises primarily from the fixed centroid-based learning approach employed by these methods. As illustrated in Figure 1, discrepancies often exist between the distributions of the source and target domains. Consequently, the learned fixed centroids may no longer be suitable for the target domain, leading to suboptimal clustering results. However, the process of training a new model from scratch for each domain incurs a substantial computational burden. More importantly, the acquired knowledge pertaining to the intra- and inter-clusters structure and patterns remains underutilized,

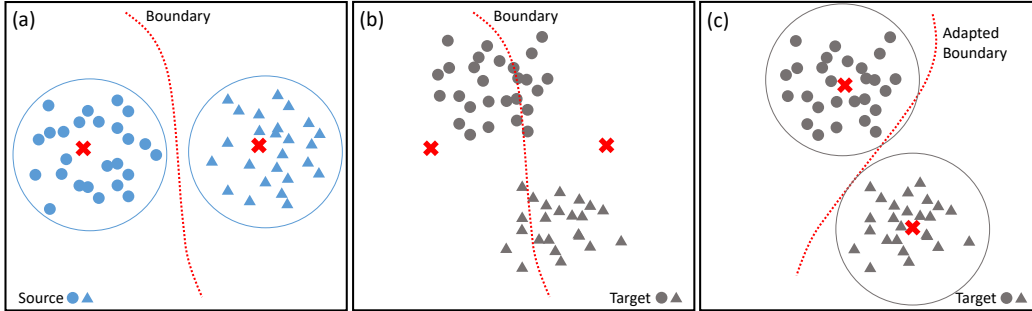


Figure 1: Problem of interest. (a) The cluster centroids learned from source domain can perfectly cluster source data samples; (b) The fixed centroids are not reliable to cluster target samples due to the distribution shift between source samples and target samples; (c) The cluster centroids are adapted to optimal position to better cluster the target samples. *Best viewed in color.*

impeding its potential to guide the clustering process on new data from similar domains. These limitations significantly hinder the practicability of deep clustering methods.

To address these limitations, there is a need for transferable deep clustering models that can leverage acquired knowledge from trained domains to guide clustering in new domains. By transferring the underlying principles of clustering on trained source domains, the model could learn how to cluster better and adapt such knowledge to clustering new data in the target domains. Unfortunately, there exists no trivial way to directly generalize existing deep clustering methods due to several major challenges: (1) **Difficulty in unsupervisedly learning the shared knowledge among different domains.** In clustering scenarios, where labeled data is unavailable, extracting meaningful and transferable knowledge that capture the commonalities of underlying cluster structures across domains is challenging. (2) **Difficulty in ensuring the learned knowledge can be adapted and customized to target domains.** As shown in Figure 1(b), the distribution discrepancies between source and target domains can significantly harm the clustering performance of existing deep clustering models. Adapting the shared knowledge to new domains remains a challenging task in order to mitigate the negative impact of these distribution discrepancies. (3) **Difficulty in theoretically ensuring a stable learning process of clustering module.** Unlike supervised learning tasks, clustering models lack labeled data to provide guidance during training, making it even more crucial to establish theoretical guarantees for stability. Addressing this challenge requires developing theoretical frameworks that can provide insights into the stability and convergence properties of clustering algorithms.

In order to address the above mentioned challenges, in this paper we propose a novel method named **Transferable Deep Clustering Model (TDCM)**. To address the first challenge, we introduce an end-to-end learning framework that can jointly optimize the feature extraction encoder and a learnable clustering module. This framework aims to leverage the learned model parameter to capture the shared intra-cluster and inter-cluster structure derived from trained cluster patterns. Therefore, the shared knowledge can be effectively transferred to unseen data from new domains. To solve the second challenge, in stead of optimizing a fixed set of centroids, a novel learnable attention-based module is proposed for the clustering process to automatically adapt centroids to the new domains, as illustrated in the Figure 1(c). Therefore, the learned clustering model is not limited to the trained source domains and can be easily generalized to other domains. Specifically, this module enables the updating of centroids through a cluster-driven bi-partite attention block, allowing the model to be aware of the similarity relationships among data samples and capture the underlying structures and patterns. Furthermore, we provide theoretical evidence to demonstrate the strong expressive power of the proposed attention-based module in representing the relationships among data samples. Our theoretical analysis reveals that traditional centroid-based clustering models like  $k$ -means or GMM can be considered as special cases of our model. This theoretical proof highlights the enhanced capabilities of our approach compared to traditional clustering methods, emphasizing its potential for mining complex cluster patterns from data. Finally, we demonstrate the effectiveness of our proposed framework on both synthetic and real-world datasets. The experimental results show that our method can achieve strongly competitive clustering performance on unseen data by a single forward pass.

## 2 Related Works

**Deep clustering models.** Existing deep clustering methods can be classified into two main categories: separately and jointly optimization. The separately optimization methods typically first train a feature extractor by self-supervised task such as deep autoencoder models, then traditional clustering methods such as  $k$ -means [10], GMM [37] or spectral clustering [1] are applied to obtain the clustering results. There are also some works [27] using density-based clustering algorithm such as DBSCAN [26] to avoid an explicit choice of number of centroids. However, the separately methods require a two-step optimization which lack the ability to train the model in an end-to-end manner to learning representation that is more suitable for clustering. On the contrary, the jointly methods are becoming more popular in the era of deep learning. One prominent approach is the Deep Embedded Clustering (DEC) model [33], which leverages an autoencoder network to map data to a lower-dimensional representations and then optimize the clustering loss KL-divergence between the soft assignments of data to centroids and an adjusted target distribution with concentrated cluster assignments. Deep clustering model (DCN) [35] jointly optimize the dimensionality reduction and  $k$ -means clustering objective functions via learning a deep autoencoder and a set of  $k$ -means centroids in the embedding space. JULE [36] formulates the joint learning in a recurrent framework, which incorporates agglomerative clustering technique as a forward pass in neural networks. More recently, some works [15, 34, 24] also propose to use contrastive learning by data augmentation techniques to obtain more discriminative representations for downstream clustering tasks.

However, most existing deep clustering methods focus on optimizing a fixed set of centroids, which limits their transferability as they struggle to handle distribution drift between different source and target domains. In contrast, our proposed model takes a different approach by adapting the centroids to learned latent embeddings, allowing it to be aware of distribution drift between domains and enhance its transferability.

**Attention models.** Attention models [2, 29, 8] have gained significant attention in the field of deep learning, revolutionizing various tasks across natural language processing, computer vision, and sequence modeling. These works collectively demonstrate the versatility and effectiveness of attention models in capturing informative relationships between data samples.

**Deep metric learning.** Our method is also related to deep metric learning methods that aim to learn representations from high-dimensional data in such a way that the similarity or dissimilarity between samples can be accurately measured. One prominent approach is the Contrastive Loss [7], which encourages similar samples to have smaller distances in the embedding space. Siamese networks [5] learns embeddings by comparing pairs of samples and optimizing the contrastive loss. More recently, the Angular Loss [31] incorporates angular margins to enhance the discriminative power of the learned embeddings. Proxy-NCA [21] employs proxy vectors to approximate the intra-class variations, enabling large-scale metric learning.

**Connection with Unsupervised Domain Adaption (UDA) methods.** While both our work and existing Unsupervised Domain Adaptation (UDA) methods [6, 18, 16] involve transferring models from source domains to target domains, the primary goal of our paper differs significantly from UDA tasks. UDA methods assume the presence of labeled data in the source domains, allowing the model to be trained in a supervised manner. In contrast, our paper focuses on a scenario where no labels are available in the source domain, necessitating the use of unsupervised learning techniques. This key distinction highlights the unique challenges and approaches we address in our research.

## 3 Preliminaries

In this section, we first formally define the problem formulation of transferable clustering task and then present the key challenges involved in designing an effective transferable deep clustering model.

In our study, we focus on a collection of datasets denoted as  $\mathcal{D} = \{D_1, D_2, \dots, D_m\}$ . Each dataset  $D_j$  is sampled from a joint probability distribution  $p(\mathcal{D})$ . Within each sampled dataset  $D_j$ , we have a set of high-dimensional feature vectors denoted as  $D_j = \{\mathbf{x}_i^j\}_{i=1}^{N_j}$ , where  $\mathbf{x}_i^j$  represents the feature vector for the  $i$ -th sample. Our objective is to learn shared knowledge in clustering from a subset of datasets, referred to as the training set  $D_s$  (source), and utilize this acquired knowledge to predict the clustering patterns on newly sampled unseen datasets, serving as the test set  $D_t$  (target).

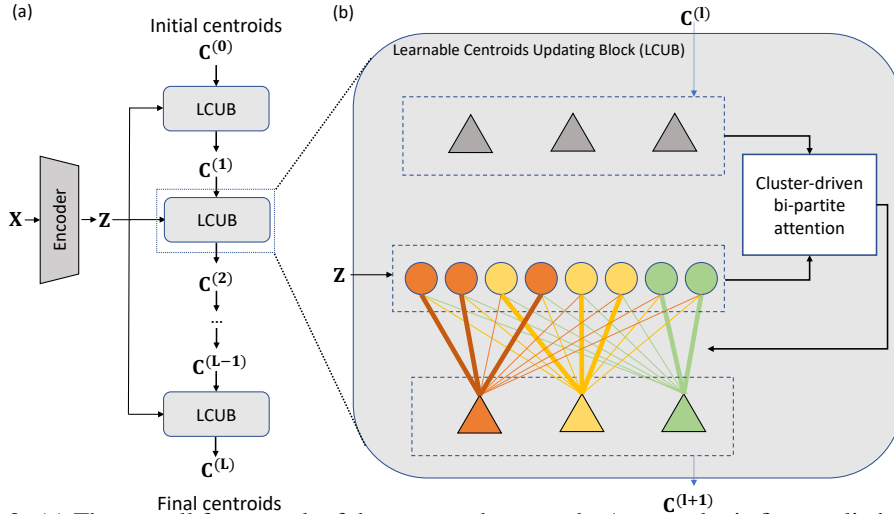


Figure 2: (a) The overall framework of the proposed approach. An encoder is first applied to extract latent embeddings  $\mathbf{Z}$  from input samples  $\mathbf{X}$ . Then the initial centroids will forward pass a series of Learnable Centroids Updating Block (LCUB) to learn the underlying similarities with centroids to reveal the cluster patterns; (b) The detailed architecture of LCUB. The current centroids  $\mathbf{C}^{(l)}$  and latent sample embeddings  $\mathbf{Z}$  are forwarded to form a bi-partite graph to calculate the assignment weights by pairwise attention scores, then the centroids are updated by the computed assignment weights.

To achieve this, we aim to learn a clustering model denoted as  $f$ , trained on the source datasets  $D_s$ . The model  $f$  partitions each source dataset  $\{\mathbf{x}_i^s\}_{i=1}^{N_s}$  into  $K$  clusters in an unsupervised manner, where  $K$  is the desired number of clusters. Our goal is to maximize the intra-cluster similarities and minimize the inter-cluster similarities by learning the clustering rule from the training datasets. Subsequently, we evaluate the clustering performance of the learned function  $f$  on the test target sets  $D_t$ . By leveraging the knowledge acquired during training, we aim to accurately predict the cluster patterns in the test datasets.

## 4 Methodology

To address the aforementioned challenges, we propose a novel method named **Transferable Deep Clustering Model (TDCM)**. To ensure the shared clustering knowledge among domains can be learned unsupervisedly, we propose an end-to-end learning framework that jointly optimizes the feature extraction encoder and a learnable clustering module, as depicted in Figure 2(a). The framework aims to utilize the learned model parameters to capture the shared intra-cluster and inter-cluster structure derived from trained cluster patterns. Consequently, this enables effective transfer of the shared knowledge to unseen data from new domains. To adjust the learned knowledge to the target domains, instead of optimizing a fixed set of centroids, a novel learnable attention-based module is proposed to automatically adapt centroids to the new domains, as shown in Figure 2(b). Therefore, the learned clustering model is not restricted to the trained source domains and can be easily generalized to other domains. Specifically, this module integrates a cluster-driven bi-partite attention block to update centroids, considering the similarity relationships among data samples and capturing underlying structures and patterns. Furthermore, we provide theoretical evidence to demonstrate the strong expressive power of the proposed attention-based module in representing the relationships among data samples. Our theoretical analysis reveals that traditional centroid-based clustering models like  $k$ -means or GMM can be considered as special cases of our model. This theoretical proof highlights the enhanced capabilities of our approach compared to traditional clustering methods, emphasizing its potential for mining complex cluster patterns from data.

### 4.1 Transferrable cluster centroids learning framework

As previously discussed, existing deep clustering models typically treat centroids as fixed learnable parameters, which limits their ability to generalize effectively to unseen data. To address this limitation, we propose a novel clustering framework that can dynamically adjust the centroids based

on the extracted sample embeddings. Consequently, the centroids are dynamically adapted based on the distribution of sample embeddings, endowing the model with the capability to effectively transfer to new domains. As depicted in Figure 2(a), an encoder  $g$  is first utilized to extract latent embeddings  $\mathbf{Z} = g_\phi(\mathbf{X}; \phi)$ . Then the adaption process involves forward pass on a series of centroids updating blocks:  $\{\mathbf{c}_j^{(0)}\}_{j=1}^K \rightarrow \{\mathbf{c}_j^{(1)}\}_{j=1}^K \rightarrow \dots \rightarrow \{\mathbf{c}_j^{(L)}\}_{j=1}^K$ , where each block consists of two steps: assignment and update. In the assignment step of the  $l$ -th ( $l \in [0, L]$ ) block, we compute the probability  $\delta_{ij}$  that assigns the data sample  $\mathbf{z}_i$  to the current cluster centroid  $\mathbf{c}_j^{(l)}$  using a score function  $\ell(\mathbf{z}_i, \mathbf{c}_j^{(l)})$ , which captures the underlying similarity relationships among samples. Subsequently, we update the cluster centroids based on the assigned data points. The updating process can be mathematically formalized as:

$$\begin{aligned} \mathbf{c}_j^{(l+1)} &= \frac{1}{\sum_i^N \sum_j^K \delta_{ij}^{(l+1)}} \sum_{i=1}^N \delta_{ij}^{(l+1)} \mathbf{z}_i, \\ \delta_{ij}^{(l+1)} &= \frac{\exp(\ell(\mathbf{z}_i, \mathbf{c}_j^{(l)})/\tau)}{\sum_{j=1}^K \exp(\ell(\mathbf{z}_i, \mathbf{c}_j^{(l)})/\tau)}, \end{aligned} \quad (1)$$

where  $\tau$  denotes the temperature hyper-parameter.

## 4.2 Learnable centroids updating module

Given the overall updating procedure described earlier, a key consideration is the choice of the score function  $\ell(\mathbf{z}_i, \mathbf{c}_j)$  to capture the similarity relationship between samples and centroids, thereby capturing the underlying cluster structure. Traditionally, a common approach is to use handcrafted score functions like the Euclidean distance  $\ell(\mathbf{z}_i, \mathbf{c}_j) = \|\mathbf{z}_i - \mathbf{c}_j\|_2$ . However, designing a specific score function requires domain knowledge and lacks generalizability across different domains.

To address this issue, we propose a learnable score function  $\ell(\mathbf{z}_i, \mathbf{c}_j; \mathbf{W})$  by introducing learnable weights  $\mathbf{W}$  that automatically capture the relational metrics between samples in a data-driven manner. Notably, the formulation in Equation 1 resembles a bi-partite graph structure of centroids and samples, which is illustrated in Figure 2(b). An attention-like mechanism, which selectively allocates resources based on the relevance of information, can be constructed based on the bi-partite structure. Since the goal of updating centroids is to gradually push centroids to represent a group of similar samples, ideally the score function  $\ell(\mathbf{z}_i, \mathbf{c}_j; \mathbf{W})$  should achieve its maximum value when  $\mathbf{z}_i = \mathbf{c}_j$ . However, a common design of attention mechanism can not guarantee this property due to the arbitrary choice of learnable parameters  $\mathbf{W}$  (see our proof in Appendix Theorem A.1).

To solve this issue from a theoretical perspective, we propose a novel clustering-driven bi-partite attention module with appropriate constraints on the parameters of learnable matrices. Specifically, the score function is designed as  $\ell(\mathbf{z}_i, \mathbf{c}_j; \mathbf{W}_Q, \mathbf{W}_K) = -\sigma(\mathbf{W}_Q(\mathbf{z}_i - \mathbf{c}_j^{(l)}) \cdot \mathbf{W}_K(\mathbf{z}_i - \mathbf{c}_j^{(l)}))/\tau$  with two learnable weight matrices and we rewrite the Equation 1 as:

$$\begin{aligned} \delta_{ij}^{(l+1)} &= \frac{\exp(-\sigma(\mathbf{W}_Q(\mathbf{z}_i - \mathbf{c}_j^{(l)}) \cdot \mathbf{W}_K(\mathbf{z}_i - \mathbf{c}_j^{(l)}))/\tau)}{\sum_{j=1}^K \exp(-\sigma(\mathbf{W}_Q(\mathbf{z}_i - \mathbf{c}_j^{(l)}) \cdot \mathbf{W}_K(\mathbf{z}_i - \mathbf{c}_j^{(l)}))/\tau)}, \\ \mathbf{W}_Q &= \mathbf{W}_Q^\top, \mathbf{W}_K = \mathbf{W}_K^\top, \end{aligned} \quad (2)$$

where  $\mathbf{W}_Q$  and  $\mathbf{W}_K$  are two learnable real-symmetric matrices and  $\sigma$  is a continuous non-decreasing nonlinear activation function (e.g. ReLU [22] or LeakyReLU [19]).

**Theorem 4.1.** *The score function  $\ell(\mathbf{z}_i, \mathbf{c}_j; \mathbf{W}_Q, \mathbf{W}_K) = -\sigma(\mathbf{W}_Q(\mathbf{z}_i - \mathbf{c}_j^{(l)}) \cdot \mathbf{W}_K(\mathbf{z}_i - \mathbf{c}_j^{(l)}))/\tau$  defined in Equation 2 can guarantee that  $\forall \mathbf{z}_i \in \mathbb{R}^b$ , we have  $\ell(\mathbf{z}_i, \mathbf{c}_j) \leq \ell(\mathbf{c}_j, \mathbf{c}_j)$ .*

*Proof.* We first define  $\mathbf{p} = \mathbf{z}_i - \mathbf{c}_j^{(l)}$  and rewrite the score function as  $\ell = -\sigma(\mathbf{W}_Q \mathbf{p} \cdot \mathbf{W}_K \mathbf{p})/\tau$ . We rewrite the inner product part as

$$\mathbf{W}_Q \mathbf{p} \cdot \mathbf{W}_K \mathbf{p} = (\mathbf{p} \mathbf{W}_Q)^\top \cdot \mathbf{W}_K \mathbf{p} = \mathbf{p}^\top (\mathbf{W}_Q^\top \mathbf{W}_K) \mathbf{p}.$$

Since  $\mathbf{W}_Q$  and  $\mathbf{W}_K$  are two real-symmetric matrices,  $\mathbf{W}_Q^\top \mathbf{W}_K$  is a positive-definite matrix. For any nonzero real vector  $\mathbf{p}$ , we have  $\mathbf{p}^\top (\mathbf{W}_Q^\top \mathbf{W}_K) \mathbf{p} > 0$ . In addition, due to the property of continuous

and non-decreasing, the nonlinear activation function would not change the ordering of values. Therefore, for all  $\mathbf{z}_i \in \mathbb{R}^b$ , we have  $\ell(\mathbf{z}_i, \mathbf{c}_j) \leq \ell(\mathbf{c}_j, \mathbf{c}_j)$ .  $\square$

In addition to theoretical property that our centroids updating module can group similar samples within same clusters, we further prove that our defined score function in Equation 2 can theoretically have stronger expressive power in representing the similarity relationship between data samples than traditional clustering technique such as  $k$ -means or GMM by the following theorems:

**Theorem 4.2.** *The score function of  $k$ -means and GMM models are special cases of our defined score function  $\ell(\mathbf{z}_i, \mathbf{c}_j; \mathbf{W}_Q, \mathbf{W}_K)$  in Equation 2.*

The proof for  $k$ -means algorithm is straightforward given here and the proof for GMM models can be found in the Appendix.

*Proof.* By setting the nonlinear function  $\sigma$  as identity function and both  $\mathbf{W}_Q$  and  $\mathbf{W}_K$  as identity matrix  $\mathbf{I}$ , we can rewrite the score function as  $\ell(\mathbf{z}_i, \mathbf{c}_j) = -\|\mathbf{z}_i - \mathbf{c}_j\|_2^2/\tau$ , which is the negative squared Euclidean distance. Then the model is equalize to a soft  $k$ -means centroids updating step. By setting  $\tau \rightarrow 0^+$ , the process converges to the traditional  $k$ -means algorithm.  $\square$

### 4.3 Unsupervised learning objective function

In order to optimize the parameters of the proposed model, the overall objective function of our framework can be written as:

$$\min_{g_\phi, \mathbf{W}_Q, \mathbf{W}_K} \mathcal{L}_{\text{clustering}} + \beta \mathcal{L}_{\text{entropy}}. \quad (3)$$

Here the first term  $\mathcal{L}_{\text{clustering}}$  is aimed at maximizing the similarity scores within clusters:

$$\begin{aligned} \mathcal{L}_{\text{clustering}} &= - \sum_l \alpha^{(l)} \sum_i^N \sum_j^K \delta_{ij}^{(l)} \ell(g_\phi(\mathbf{x}_i), \mathbf{c}_j^{(l)}; \mathbf{W}_Q, \mathbf{W}_K), \\ \text{s.t. } \mathbf{W}_Q \mathbf{W}_Q^T &= \mathbf{I}, \mathbf{W}_K \mathbf{W}_K^T = \mathbf{I} \end{aligned} \quad (4)$$

where  $\alpha^{(l)}$  are hyperparameters to tune the balance between blocks and orthogonal constraints are incorporated to prevent the trivial solution of scale changes in the embeddings. We can treat the constraints as a Lagrange multiplier and solve an equivalent problem by substituting the constraint to a regularization term.

Besides the clustering loss term, the entropy loss term is aimed at avoiding the trivial solution of assigning all samples to one single cluster:

$$\begin{aligned} \mathcal{L}_{\text{entropy}} &= - \sum_l \alpha^{(l)} \sum_j^K \pi_j^{(l)} \log \pi_j^{(l)}, \\ \pi_j^{(l)} &= \sum_i \delta_{ij}^{(l)} = \sum_i \frac{\exp(-\sigma(\mathbf{W}_Q(\mathbf{z}_i - \mathbf{c}_j^{(l-1)}) \cdot \mathbf{W}_K(\mathbf{z}_i - \mathbf{c}_j^{(l-1)}))/\tau)}{\sum_{j=1}^K \exp(-\sigma(\mathbf{W}_Q(\mathbf{z}_i - \mathbf{c}_j^{(l-1)}) \cdot \mathbf{W}_K(\mathbf{z}_i - \mathbf{c}_j^{(l-1)}))/\tau)}, \end{aligned} \quad (5)$$

where  $\pi_j^{(l)}$  reflects the size of each clusters.

**Initialization of centroids.** Many previous studies use the centroids provided by traditional clustering methods such as  $k$ -means on the latent embeddings as the initialization of centroids. However, these methods usually requires to load all data samples into the memory, which can be hardly generalize to a mini-batch version due to the permutation invariance of cluster centroids. To solve this issue, we propose to initialize the centroids  $\{\mathbf{c}_j^{(0)}\}_{j=1}^K$  before blocks as a set of orthogonal vectors in the embedding space, e.g. identity matrix  $\mathbf{I}$ .

### 4.4 Complexity analysis

Here we present the complexity analysis of our proposed dynamic centroids update module. In each block, we need to compute the pair-wise scores between centroids and data samples in Equation 2.

Assuming the embedding space dimension is denoted as  $b$ , the time complexity to calculate the score functions in one block is  $O(NKb^2)$ . Consequently, performing  $L$  blocks would entail a time complexity of  $O(LNKb^2)$ , where  $N$  represents the number of samples and  $K$  denotes the number of centroids. It is important to note that our framework naturally supports a mini-batch version, which significantly enhances the scalability of the model and improves its efficiency.

## 5 Experiments

In this section, the experimental settings are introduced first in Section 5.1, then the performance of the proposed method on synthetic datasets are presented in Section 5.2. We further present the effectiveness test on our method against distributional shift between domains on real-world datasets in Section 5.3. In addition, we verify the effectiveness of framework components through ablation studies in Section 5.4 and measure the parameter sensitivity in Appendix B.2 due to space limit.

### 5.1 Experimental settings

**Synthetic datasets.** In order to assess the generalization capability of our proposed method towards unseen domain data, we conduct an evaluation using synthetic datasets. A source domain is first generated by sampling  $K$  equal-sized data clusters. The data features are sampled from multi-Gaussian distributions with randomized centers and covariance matrices, which is similar to previous works [11, 4]. Subsequently, a corresponding target domain is created by randomly perturbing the centers of the source domain clusters. This ensures the presence of distributional drift between the train and test set data. To provide comprehensive results, we vary the value of  $K$  and generate 10 distinct datasets for each value of  $K$ . We train the clustering model on source domain and test on the target domain. Our experimental results are reported as an average of 5 runs on each dataset, with different random seeds employed to ensure robustness.

**Real-world datasets.** To further evaluate the generalization capability of our proposed method under real-world scenarios, commonly used real-world benchmark datasets are included. (1) **Digits** which includes MNIST and USPS, is a standard digit recognition benchmark that commonly used by previous studies [33, 35, 17, 16]. Follow previous works [17, 16], we train the model on the source domain training set and test the model on the target domain test set. All input images are resized to  $32 \times 32$ . (2) **CIFAR-10** [13] is commonly used image benchmark datasets in evaluating deep clustering models. We treat the training set as source domain and test set as target domain. We introduce CenterCrop to the test set to create distribution drift.

**Comparison methods.** We evaluate the proposed method on both synthetic and real-world benchmark datasets and compare it with both traditional clustering and state-of-the-art deep clustering techniques such as  $k$ -means, GMM, DAE [30], DAEGMM [32], DEC [33], DCN [35], JULE [36], CC [15] and IDFD [34].

**Evaluation metrics.** In our evaluation of clustering performance, we employ widely recognized metrics, namely normalized mutual information (NMI) [3], adjusted rand index (ARI) [38], and clustering accuracy (ACC) [3]. By combining NMI, ARI, and ACC, we can comprehensively demonstrate the quality and efficacy of our clustering results.

**Implementation details.** Our proposed model serves as a general framework, allowing for the integration of various commonly used deep representation learning techniques as the encoder part. To ensure a fair comparison with previous works, we enforce the use of the same encoder for feature extraction across all models. Specifically, for synthetic data, we utilize a three-layer multilayer perceptron (MLP) as the encoder. For the Digits dataset, we employ the classical LeNet-5 network [14] as the encoder. Furthermore, for the CIFAR-10 datasets, we utilize the ResNet-18 network [9] as the encoder. We use  $L = 4$  layers of blocks to update the synthetic datasets and  $L = 5$  for the real-world datasets. The temperature  $\tau$  is set as 1.0 throughout the whole experiments. We use an linearly increasing series of values for the weights  $\alpha$  for penalizing each block in loss function, where the final layer has the largest weight. We train the whole network through back-propagation and utilize Adam [12] as the optimizer. The initial learning rate is set as  $5e^{-3}$  for the synthetic datasets and  $5e^{-4}$  for the real-world datasets, and the weight decay rate is set as  $5e^{-4}$ . The total number of training

Table 1: Clustering performance on the synthetic datasets with varying number of clusters  $K$ . The models are trained on source domain and tested on target domain. We denote the performance drop from training set to test set as ‘diff’, where smaller values indicate better generalization ability. The best generalization performances are highlighted in bold.

model		$K=2$			$K=3$			$K=5$			$K=10$		
		NMI	ARI	ACC	NMI	ARI	ACC	NMI	ARI	ACC	NMI	ARI	ACC
$k$ -means	source	0.995	0.998	0.999	0.951	0.930	0.940	0.898	0.845	0.855	0.924	0.850	0.845
	target	0.622	0.596	0.828	0.883	0.846	0.916	0.750	0.653	0.745	0.782	0.643	0.731
	diff	0.373	0.402	0.171	0.068	0.084	0.024	0.148	0.192	0.110	0.142	0.207	0.114
GMM	source	0.995	0.998	0.999	0.991	0.995	0.998	0.934	0.919	0.936	0.953	0.919	0.924
	target	0.622	0.597	0.824	0.902	0.877	0.948	0.756	0.674	0.775	0.788	0.661	0.755
	diff	0.373	0.401	0.175	0.089	0.118	0.050	0.178	0.245	0.161	0.165	0.258	0.169
AE	source	0.995	0.998	0.999	0.949	0.928	0.939	0.899	0.852	0.861	0.919	0.855	0.854
	target	0.532	0.516	0.778	0.754	0.746	0.824	0.642	0.635	0.701	0.702	0.613	0.712
	diff	0.463	0.482	0.221	0.195	0.182	0.115	0.257	0.217	0.160	0.217	0.242	0.142
DAEGMM	source	0.996	0.998	0.998	0.990	0.993	0.989	0.933	0.922	0.933	0.945	0.908	0.916
	target	0.522	0.507	0.713	0.842	0.827	0.878	0.696	0.704	0.734	0.690	0.610	0.687
	diff	0.474	0.491	0.285	0.148	0.166	0.111	0.237	0.218	0.199	0.255	0.298	0.229
DEC	source	0.995	0.998	0.999	0.989	0.991	0.997	0.932	0.942	0.978	0.955	0.942	0.973
	target	0.692	0.636	0.828	0.889	0.851	0.905	0.766	0.683	0.785	0.701	0.605	0.713
	diff	0.303	0.362	0.171	0.100	0.140	0.092	0.166	0.259	0.193	0.254	0.337	0.260
DCN	source	0.994	0.997	0.999	0.991	0.991	0.997	0.937	0.950	0.982	0.963	0.954	0.978
	target	0.654	0.498	0.719	0.703	0.608	0.795	0.643	0.698	0.742	0.689	0.599	0.753
	diff	0.340	0.499	0.280	0.288	0.383	0.202	0.294	0.252	0.240	0.274	0.355	0.225
CC	source	0.990	0.992	0.998	0.980	0.981	0.998	0.938	0.950	0.981	0.962	0.963	0.982
	target	0.578	0.555	0.694	0.821	0.802	0.854	0.623	0.634	0.701	0.694	0.645	0.721
	diff	0.412	0.437	0.304	0.159	0.179	0.144	0.315	0.316	0.280	0.268	0.318	0.261
TDCM	source	0.990	0.991	0.998	0.975	0.982	0.994	0.935	0.949	0.979	0.961	0.965	0.984
	target	0.989	0.995	0.999	0.953	0.957	0.984	0.901	0.896	0.951	0.885	0.863	0.925
	diff	<b>0.001</b>	<b>-0.004</b>	<b>-0.001</b>	<b>0.022</b>	<b>0.025</b>	<b>0.010</b>	<b>0.034</b>	<b>0.053</b>	<b>0.028</b>	<b>0.076</b>	<b>0.102</b>	<b>0.059</b>

epochs is 500 for the synthetic datasets and 2,000 for the real-world datasets. The batch size is set as 256 for synthetic and DIGITS datasets, and 128 for CIFAR-10 dataset. Data augmentation techniques are added like previous papers [15, 34] for the purpose of training discriminative representations for all the image datasets. The experiments are carried out on NVIDIA A6000 GPUs, which takes around 30 gpu-hours to train the model on CIFAR-10 dataset.

## 5.2 Synthetic data results

Table 1 presents the clustering performance on both the trained source domain and test target domain of synthetic datasets. The results show the remarkable effectiveness of our proposed TDCM framework in achieving superior generalization performance when transferring the trained model from source to target sets across all synthetic scenarios. Specifically, TDCM consistently outperforms all the comparison methods, exhibiting an average improvement of 0.215, 0.243, and 0.157 on NMI, ARI, and ACC metrics, respectively. Notably, the performance of the TDCM model on the test set exhibits only a marginal average decrease of 0.033, 0.044, and 0.024 on NMI, ARI, and ACC metrics, respectively, compared to the training set. These results provide strong evidence that our proposed method significantly enhances the transferability of the clustering model, demonstrating its superior performance and robustness. On the other hand, although the comparison methods can achieve competitive performance on the trained training set, their performance drops significantly when transfer from source to target domains, which proves that their fixed set of optimized centroids can not handle the distribution drift between domains.

## 5.3 Real-world data results

We report the clustering results of the real-world datasets in Table 2. The results demonstrate the strength of our proposed TDCM framework by consistently achieving the best performance when test on test sets across all datasets. Specifically, TDCM consistently outperforms all the comparison methods, exhibiting an average improvement of 0.206, 0.342, 0.439 on MNIST, USPS, and CIFAR-10 data test sets, respectively. Our results strongly demonstrate the enhanced transferability of our proposed method for the clustering model, highlighting its superior performance. It worth noting that the improvement of our model on CIFAR-10 dataset is more significant than the other two digits dataset. A possible reason is CIFAR-10 datasets are more complex than the other two datasets, which may prove that our model can handle complex data with high dimensional features.



Table 2: Clustering performance on the real-world datasets. The models are trained on source domain and tested on target domain. The best performances on test datasets are highlighted in bold.

model	$k$ -means	GMM		AE		DEC		DCN		JULE		CC		IDFD		TDCM			
		source	target	source	target	source	target	source	target	source	target	source	target	source	target	source	target		
MNIST	NMI	0.503	0.432	0.466	0.387	0.808	0.774	0.804	0.789	0.811	0.779	0.913	0.874	0.932	0.881	0.921	0.898	0.925	<b>0.933</b>
	ARI	0.476	0.382	0.398	0.343	0.765	0.698	0.789	0.764	0.768	0.730	0.874	0.849	0.873	0.864	0.88	0.841	0.873	<b>0.886</b>
	ACC	0.535	0.501	0.465	0.431	0.797	0.754	0.849	0.822	0.831	0.818	0.963	0.907	0.945	0.895	0.951	0.931	0.938	<b>0.958</b>
USPS	NMI	0.607	0.496	0.633	0.451	0.593	0.446	0.582	0.387	0.856	0.495	0.881	0.872	0.902	0.652	0.913	0.754	0.905	<b>0.911</b>
	ARI	0.597	0.503	0.623	0.402	0.549	0.389	0.565	0.234	0.834	0.324	0.858	0.840	0.889	0.613	0.901	0.746	0.885	<b>0.879</b>
	ACC	0.611	0.587	0.654	0.558	0.610	0.537	0.605	0.451	0.869	0.598	0.913	0.783	0.908	0.705	0.937	0.803	0.925	<b>0.910</b>
CIFAR-10	NMI	0.087	0.076	0.095	0.084	0.239	0.143	0.257	0.143	0.243	0.124	0.192	0.108	0.705	0.548	0.711	0.578	0.687	<b>0.664</b>
	ARI	0.049	0.033	0.062	0.049	0.169	0.114	0.161	0.094	0.143	0.079	0.138	0.087	0.637	0.421	0.663	0.467	0.642	<b>0.617</b>
	ACC	0.229	0.178	0.253	0.230	0.314	0.251	0.301	0.231	0.275	0.194	0.272	0.201	0.790	0.620	0.815	0.639	0.795	<b>0.773</b>

Table 3: Ablation studies. Values in parentheses indicate standard deviation.

		Synthetic K=2			Synthetic K=5			CIFAR-10		
		NMI	ARI	ACC	NMI	ARI	ACC	NMI	ARI	ACC
Full model	source	0.990(0.018)	0.991(0.013)	0.998(0.001)	0.935(0.001)	0.949(0.001)	0.979(0.001)	0.687(0.045)	0.642(0.041)	0.795(0.032)
	target	0.989(0.017)	0.995(0.007)	0.999(0.002)	0.901(0.035)	0.896(0.026)	0.951(0.013)	0.664(0.061)	0.617(0.057)	0.773(0.043)
variant-R	source	0.992(0.016)	0.991(0.015)	0.997(0.001)	0.926(0.014)	0.935(0.015)	0.978(0.008)	0.276(0.172)	0.240(0.201)	0.359(0.135)
	target	0.678(0.234)	0.541(0.301)	0.698(0.197)	0.754(0.123)	0.721(0.141)	0.805(0.067)	0.178(0.087)	0.159(0.102)	0.246(0.155)
variant-O	source	0.987(0.023)	0.976(0.025)	0.991(0.009)	0.928(0.015)	0.935(0.017)	0.970(0.008)	0.236(0.092)	0.205(0.071)	0.272(0.045)
	target	0.878(0.064)	0.842(0.070)	0.898(0.045)	0.851(0.073)	0.821(0.091)	0.902(0.027)	0.148(0.075)	0.139(0.042)	0.186(0.055)
variant-E	source	0.993(0.012)	0.991(0.013)	0.998(0.002)	0.935(0.001)	0.949(0.001)	0.975(0.004)	0.547(0.120)	0.492(0.141)	0.655(0.102)
	target	0.969(0.037)	0.955(0.039)	0.981(0.012)	0.891(0.025)	0.886(0.031)	0.936(0.020)	0.564(0.161)	0.417(0.134)	0.597(0.143)

## 5.4 Ablation studies

Here we investigate the impact of the proposed components of TDCM. We first consider variants of removing the real-symmetric constraints and orthogonal constraints in our model, named *variant-R* and *variant-O*. In addition, we also remove the entropy loss in our overall loss function, named *variant-E*. We present the results on two synthetic datasets ( $K = 2, 5$ ) and CIFAR-10 real-world dataset in Table 3, where we can observe a significant performance drop consistently for all variants. Especially, we observe that the standard deviation of all variants are larger than the full model, especially for the *variant-R* that removes real-symmetric constraint. Such behavior may demonstrate the importance of these proposed constraints in guaranteeing a stable training process, which is highly consistent with our theoretical analysis.

## 5.5 Visualization of centroids updating process

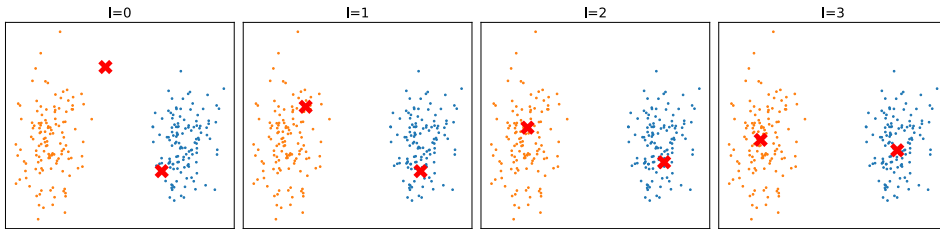


Figure 3: A visualization of centroids updating process with  $L = 3$  blocks. Here orange and blue points denote two clusters and the red point denotes the centroids.

In order to illustrate the learned centroids updating behavior by our designed module, here we visualize the layer-wise updated centroids in  $K = 2$  synthetic dataset test set in Figure 3. From the visualization we can observe that by forward passing the updating blocks, the centroids are adapted to a more clear cluster structure by the learned similarity metrics. It worth noting that the final adapted centroids are not necessarily at the ‘center’ of the clusters, which demonstrate that the designed module can automatically find the underlying similarity metric between samples that is suitable for the given data.

## 6 Conclusions and Limitations

In this study, we introduce a novel framework called **Transferable Deep Clustering Model (TDCM)** to tackle the challenge of limited generalization ability in previous end-to-end deep clustering techniques when faced with unseen domain data. In stead of optimizing a fixed set of centroids specific to the training source domain, our proposed TDCM employs an adapted centroids updating module, enabling automatic adaptation of centroids based on the input domain data. As a result, our framework exhibits enhanced generalization capabilities to handle unseen domain data. To capture the intrinsic structure and patterns of clusters, we propose an attention-based learnable module, which learns

a data-driven score function for measuring the underlying similarity among samples. Theoretical analysis guarantees the effectiveness of our proposed module in extracting underlying similarity relationships, surpassing conventional clustering techniques such as  $k$ -means or Gaussian Mixture Models (GMM) in terms of expressiveness. Extensive experiments conducted on synthetic and real-world datasets validate the effectiveness of our proposed model in addressing distributional drift during the transfer of clustering knowledge from trained source domains to unseen target domains.

We acknowledge certain limitations associated with our proposed framework. One limitation is that our TDCM is a centroids-based method, similar to previous centroids-based methods like  $k$ -means, GMM, DEN, DEC, DCN, CC, and IDFD, which necessitates a predefined number of clusters for the model. An inappropriate choice of the number of clusters can adversely affect the performance of the model. Additionally, our adapted updating module requires the updating matrix to be real-symmetric, implying that the hidden dimension of clusters should remain fixed throughout the adaptation process. However, as the primary objective of this work is to pioneer deep clustering models for transfer learning across different domains and propose a practical solution to address this problem, the aforementioned challenges certainly go beyond the scope of this study. Nevertheless, we consider these challenges as potential avenues for future research.

## References

- [1] Séverine Affeldt, Lazhar Labiod, and Mohamed Nadif. Spectral clustering via ensemble deep autoencoder learning (sc-edae). *Pattern Recognition*, 108:107522, 2020.
- [2] Dzmitry Bahdanau, Kyunghyun Cho, and Yoshua Bengio. Neural machine translation by jointly learning to align and translate. *arXiv preprint arXiv:1409.0473*, 2014.
- [3] Deng Cai, Xiaofei He, and Jiawei Han. Locally consistent concept factorization for document clustering. *IEEE Transactions on Knowledge and Data Engineering*, 23(6):902–913, 2010.
- [4] Ricky TQ Chen, Yulia Rubanova, Jesse Bettencourt, and David K Duvenaud. Neural ordinary differential equations. *Advances in neural information processing systems*, 31, 2018.
- [5] Sumit Chopra, Raia Hadsell, and Yann LeCun. Learning a similarity metric discriminatively, with application to face verification. In *2005 IEEE Computer Society Conference on Computer Vision and Pattern Recognition (CVPR'05)*, volume 1, pages 539–546. IEEE, 2005.
- [6] Yaroslav Ganin and Victor Lempitsky. Unsupervised domain adaptation by backpropagation. In *International conference on machine learning*, pages 1180–1189. PMLR, 2015.
- [7] Raia Hadsell, Sumit Chopra, and Yann LeCun. Dimensionality reduction by learning an invariant mapping. In *2006 IEEE Computer Society Conference on Computer Vision and Pattern Recognition (CVPR'06)*, volume 2, pages 1735–1742. IEEE, 2006.
- [8] Kai Han, Yunhe Wang, Hanting Chen, Xinghao Chen, Jianyuan Guo, Zhenhua Liu, Yehui Tang, An Xiao, Chunjing Xu, Yixing Xu, et al. A survey on vision transformer. *IEEE transactions on pattern analysis and machine intelligence*, 45(1):87–110, 2022.
- [9] Kaiming He, Xiangyu Zhang, Shaoqing Ren, and Jian Sun. Deep residual learning for image recognition. In *Proceedings of the IEEE conference on computer vision and pattern recognition*, pages 770–778, 2016.
- [10] Peihao Huang, Yan Huang, Wei Wang, and Liang Wang. Deep embedding network for clustering. In *2014 22nd International conference on pattern recognition*, pages 1532–1537. IEEE, 2014.
- [11] Fariba Karimi, Mathieu Génois, Claudia Wagner, Philipp Singer, and Markus Strohmaier. Homophily influences ranking of minorities in social networks. *Scientific reports*, 8(1):1–12, 2018.
- [12] Diederik P Kingma and Jimmy Ba. Adam: A method for stochastic optimization. *arXiv preprint arXiv:1412.6980*, 2014.
- [13] Alex Krizhevsky, Geoffrey Hinton, et al. Learning multiple layers of features from tiny images. 2009.
- [14] Yann LeCun, Léon Bottou, Yoshua Bengio, and Patrick Haffner. Gradient-based learning applied to document recognition. *Proceedings of the IEEE*, 86(11):2278–2324, 1998.

- [15] Yunfan Li, Peng Hu, Zitao Liu, Dezhong Peng, Joey Tianyi Zhou, and Xi Peng. Contrastive clustering. In *Proceedings of the AAAI Conference on Artificial Intelligence*, volume 35, pages 8547–8555, 2021.
- [16] Jian Liang, Dapeng Hu, and Jiashi Feng. Do we really need to access the source data? source hypothesis transfer for unsupervised domain adaptation. In *International Conference on Machine Learning*, pages 6028–6039. PMLR, 2020.
- [17] Mingsheng Long, Zhangjie Cao, Jianmin Wang, and Michael I Jordan. Conditional adversarial domain adaptation. *Advances in neural information processing systems*, 31, 2018.
- [18] Mingsheng Long, Han Zhu, Jianmin Wang, and Michael I Jordan. Unsupervised domain adaptation with residual transfer networks. *Advances in neural information processing systems*, 29, 2016.
- [19] Andrew L Maas, Awni Y Hannun, Andrew Y Ng, et al. Rectifier nonlinearities improve neural network acoustic models. In *Proc. icml*, volume 30, page 3. Atlanta, Georgia, USA, 2013.
- [20] Erxue Min, Xifeng Guo, Qiang Liu, Gen Zhang, Jianjing Cui, and Jun Long. A survey of clustering with deep learning: From the perspective of network architecture. *IEEE Access*, 6:39501–39514, 2018.
- [21] Yair Movshovitz-Attias, Alexander Toshev, Thomas K Leung, Sergey Ioffe, and Saurabh Singh. No fuss distance metric learning using proxies. In *Proceedings of the IEEE international conference on computer vision*, pages 360–368, 2017.
- [22] Vinod Nair and Geoffrey E Hinton. Rectified linear units improve restricted boltzmann machines. In *Proceedings of the 27th international conference on machine learning (ICML-10)*, pages 807–814, 2010.
- [23] Sameer A Nene, Shree K Nayar, Hiroshi Murase, et al. Columbia object image library (coil-20). 1996.
- [24] Chuang Niu, Hongming Shan, and Ge Wang. Spice: Semantic pseudo-labeling for image clustering. *IEEE Transactions on Image Processing*, 31:7264–7278, 2022.
- [25] Yazhou Ren, Jingyu Pu, Zhimeng Yang, Jie Xu, Guofeng Li, Xiaorong Pu, Philip S Yu, and Lifang He. Deep clustering: A comprehensive survey. *arXiv preprint arXiv:2210.04142*, 2022.
- [26] Yazhou Ren, Ni Wang, Mingxia Li, and Zenglin Xu. Deep density-based image clustering. *Knowledge-Based Systems*, 197:105841, 2020.
- [27] Alex Rodriguez and Alessandro Laio. Clustering by fast search and find of density peaks. *science*, 344(6191):1492–1496, 2014.
- [28] Chunfeng Song, Feng Liu, Yongzhen Huang, Liang Wang, and Tieniu Tan. Auto-encoder based data clustering. In *Progress in Pattern Recognition, Image Analysis, Computer Vision, and Applications: 18th Iberoamerican Congress, CIARP 2013, Havana, Cuba, November 20-23, 2013, Proceedings, Part I 18*, pages 117–124. Springer, 2013.
- [29] Ashish Vaswani, Noam Shazeer, Niki Parmar, Jakob Uszkoreit, Llion Jones, Aidan N Gomez, Łukasz Kaiser, and Illia Polosukhin. Attention is all you need. *Advances in neural information processing systems*, 30, 2017.
- [30] Pascal Vincent, Hugo Larochelle, Isabelle Lajoie, Yoshua Bengio, Pierre-Antoine Manzagol, and Léon Bottou. Stacked denoising autoencoders: Learning useful representations in a deep network with a local denoising criterion. *Journal of machine learning research*, 11(12), 2010.
- [31] Jian Wang, Feng Zhou, Shilei Wen, Xiao Liu, and Yuanqing Lin. Deep metric learning with angular loss. In *Proceedings of the IEEE international conference on computer vision*, pages 2593–2601, 2017.
- [32] Jinghua Wang and Jianmin Jiang. Unsupervised deep clustering via adaptive gmm modeling and optimization. *Neurocomputing*, 433:199–211, 2021.
- [33] Junyuan Xie, Ross Girshick, and Ali Farhadi. Unsupervised deep embedding for clustering analysis. In *International conference on machine learning*, pages 478–487. PMLR, 2016.
- [34] Kouta Nakata, Yaling Tao, Kentaro Takagi. Clustering-friendly representation learning via instance discrimination and feature decorrelation. *Proceedings of ICLR 2021*, 2021.

- [35] Bo Yang, Xiao Fu, Nicholas D Sidiropoulos, and Mingyi Hong. Towards k-means-friendly spaces: Simultaneous deep learning and clustering. In *international conference on machine learning*, pages 3861–3870. PMLR, 2017.
- [36] Jianwei Yang, Devi Parikh, and Dhruv Batra. Joint unsupervised learning of deep representations and image clusters. In *Proceedings of the IEEE conference on computer vision and pattern recognition*, pages 5147–5156, 2016.
- [37] Xu Yang, Cheng Deng, Feng Zheng, Junchi Yan, and Wei Liu. Deep spectral clustering using dual autoencoder network. In *Proceedings of the IEEE/CVF conference on computer vision and pattern recognition*, pages 4066–4075, 2019.
- [38] Ka Yee Yeung and Walter L Ruzzo. Details of the adjusted rand index and clustering algorithms, supplement to the paper an empirical study on principal component analysis for clustering gene expression data. *Bioinformatics*, 17(9):763–774, 2001.
- [39] Zheng Zhang and Liang Zhao. Unsupervised deep subgraph anomaly detection. In *2022 IEEE International Conference on Data Mining (ICDM)*, pages 753–762. IEEE, 2022.
- [40] Sheng Zhou, Hongjia Xu, Zhuonan Zheng, Jiawei Chen, Jiajun Bu, Jia Wu, Xin Wang, Wenwu Zhu, Martin Ester, et al. A comprehensive survey on deep clustering: Taxonomy, challenges, and future directions. *arXiv preprint arXiv:2206.07579*, 2022.

## A Additional Theorems

A conventional attention-like updating mechanism can be written as:

$$\delta_{ij}^{(l+1)} = \frac{\exp(\sigma(\mathbf{W}_Q \mathbf{z}_i \cdot \mathbf{W}_K \mathbf{c}_j^{(l)})/\tau)}{\sum_{j=1}^K \exp(\sigma(\mathbf{W}_Q \mathbf{z}_i \cdot \mathbf{W}_K \mathbf{c}_j^{(l)})/\tau)}, \quad (6)$$

where  $\mathbf{W}_Q$  and  $\mathbf{W}_K$  are two learnable matrices and  $\sigma$  is a nonlinear activation function.

Unfortunately, simply adopting the above commonly used attention based score function can not guarantee the similarity relationship between samples can be correctly revealed by the learned score function, which may leads to the failure of capturing the true pattern of clusters.

**Theorem A.1.** *For the score function  $\ell(\mathbf{z}_i, \mathbf{c}_j) = \sigma(\mathbf{W}_Q \mathbf{z}_i \cdot \mathbf{W}_K \mathbf{c}_j^{(l)})/\tau$  defined in Equation 6,  $\forall \mathbf{z}_i \in \mathbb{R}^b$ , an arbitrary choice of  $\mathbf{W}_Q$  and  $\mathbf{W}_K$  can not guarantee  $\ell(\mathbf{z}_i, \mathbf{c}_j) \leq \ell(\mathbf{c}_j, \mathbf{c}_j)$ .*

*Proof.* Here we give an example by discarding the nonlinear function  $\sigma$  and set the temperature  $\tau = 1$ . Let

$$\mathbf{W}_Q = \begin{pmatrix} 1 & 0 \\ 1 & 0 \end{pmatrix}, \mathbf{W}_K = \begin{pmatrix} 0 & -1 \\ 0 & -1 \end{pmatrix}, \mathbf{c}_j = \begin{pmatrix} 0 \\ -1 \end{pmatrix},$$

when  $\mathbf{z}_i = \mathbf{c}_j = \begin{pmatrix} 0 \\ -1 \end{pmatrix}$ , we have  $\ell(\mathbf{z}_i, \mathbf{c}_j) = 0$ . However, if we set  $\mathbf{z}_i = \begin{pmatrix} 1 \\ 0 \end{pmatrix}$ , we have  $\ell(\mathbf{z}_i, \mathbf{c}_j) = -2$ . Therefore,  $\ell(\mathbf{z}_i, \mathbf{c}_j) \leq \ell(\mathbf{c}_j, \mathbf{c}_j)$  does not hold  $\forall \mathbf{z}_i \in \mathbb{R}^b$ .  $\square$

In addition, we further give the mathematical proof for the Theorem 4.2 that GMM models can be considered as special cases of our method:

*Proof.* By setting the nonlinear function  $\sigma$  as identity function and the product of  $\mathbf{W}_Q$  and  $\mathbf{W}_K$  as one single positive-definite matrix  $\Sigma = \mathbf{W}_Q^\top \mathbf{W}_K$ , we can rewrite the score function as  $\ell(\mathbf{z}_i, \mathbf{c}_j) = -(\mathbf{z}_i - \mathbf{c}_j)^\top \Sigma (\mathbf{z}_i - \mathbf{c}_j) / \tau$ . The updating function is equalized to a GMM centroids updating step, while our model retains more expressive power due to the nonlinear activation function and the less-constrained parameters of matrices  $\mathbf{W}_Q$  and  $\mathbf{W}_K$ .  $\square$

## B Additional Experiments

### B.1 Additional experiments on large size classes dataset

We have carried out additional experiments using the COIL100 dataset [23], which consists of 100 distinct classes. In these experiments, the first 50 classes are used as the training source domain,

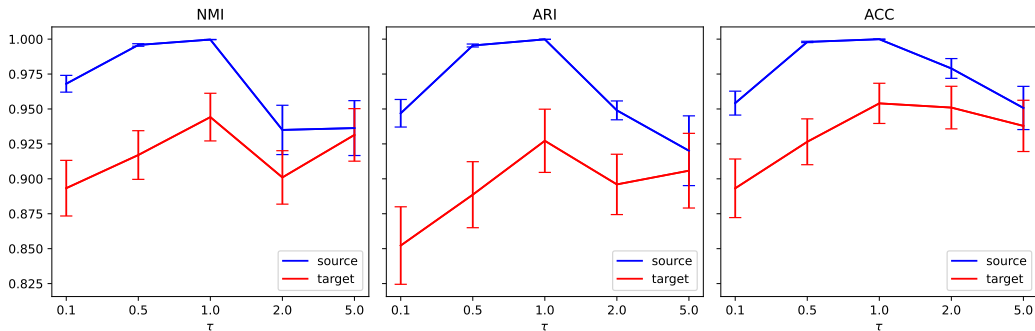
Table 4: Additional experimental results on COIL100 dataset.

Domain	$k$ -means	GMM	AE	DEC	DCN	JULE	CC	IDFD	Ours
Source	0.819	0.831	0.824	0.855	0.899	0.985	0.987	0.986	0.986
Target	0.644	0.519	0.743	0.765	0.824	0.954	0.942	0.967	<b>0.984</b>

Table 5: Additional sensitivity experiments on number of updating blocks  $L$ , weights of penalization terms on each layers  $\alpha$ , and  $\beta$ .

Original	$L = 4$	$L = 2$	$L = 8$	$L = 16$	$\alpha_{\text{linear}}$	$\alpha_{\text{last}}$	$\beta = 1$	$\beta = 0$	$\beta = 10$
Source	0.990	0.975	0.984	0.912	0.990	0.984	0.990	0.955	0.101
Target	0.989	0.974	0.987	0.910	0.989	0.988	0.989	0.972	0.098

while the remaining 50 classes serve as the test target domain. The Normalized Mutual Information (NMI) clustering results for our method and comparative techniques are presented in the Table 4. We can observe that our methods can outperform all the comparison methods on the target domain with only minor performance drop from source domain (0.002). Although state-of-the-art comparison methods such as JULE, CC and IDFD can achieve comparable results on source domain, they are notably affected by the domain shift between source and target, leading to a noticeable decline in performance.

Figure 4: The parameter sensitivity experimental results for the temperature parameter  $\tau$  from 0.1 to 5.0. Here we present the results on both trained source domain and test target domain.

## B.2 Sensitivity analysis

In this section, we include sensitivity analysis on the critical parameters that involved in our designed model, which is the temperature parameter  $\tau$  in Equation 2. In an intuitive manner, the temperature parameter significantly influences the determination of the computed distance metrics between samples. Specifically, an increased value of  $\tau$  tends to reduce the disparity between the estimated similarity scores between samples and centroids. Therefore, we vary the value of  $\tau$  from 0.1 to 5.0 to examine the sensitivity of choice on temperature. We present the results of sensitivity analysis on  $K = 5$  synthetic datasets in Figure 4. From the figure we can observe that the performance of our proposed method usually peaks at the value of  $\tau = 1.0$  for both training and test set. It is also worth noting that our proposed method is robust since the performance will stably change with the value of temperature parameter  $\tau$ . Besides, an interesting observation is that when the value of  $\tau$  is becoming larger (e.g. 5.0), the gap of performance between source and target domain decreased. A possible explanation is that a larger temperature value can smooth the discrepancy between samples, which results in a better generalizable model.

We also include additional sensitivity analysis on the hyperparameters, e.g. number of updating blocks  $L$ , weights of penalization terms on each layers  $\alpha$ , and  $\beta$  to balance the clustering loss and entropy loss. Here we use the synthetic dataset ( $K = 2$ ) for conducting the performance for the purpose of efficiency. The results are presented in Table

- (1) It is noticeable that the selection of hyperparameters can influence the training capacity within the source domain. However, the ability to generalize from the source domain to the target domain is hardly affected to these changes.
- (2) We vary the number of updating blocks  $L$  from 2 to 16. We can observe from the results that an appropriate choice of number of updating blocks can affect the training performance on the source domain. Choosing either a too small value (such as  $L = 2$ ) or a too large one (such as  $L = 16$ ) could hinder the model's ability to optimize towards the underlying optimal clustering.
- (3) We compare two choices of  $\alpha$  to tune the balance of loss between different blocks. We adopt  $\alpha_{linear}$ , which is to equally penalize the loss on each block, and  $\alpha_{last}$ , which only penalize on the last block. We observe that the performance only slightly different between these two, which indicates our model is not sensitive to the choice of  $\alpha$ .
- (4) We additionally evaluate the impact of the regularization term through the hyperparameter  $\beta$ . Our observations indicate that performance can significantly drop if the entropy regularization is eliminated ( $\beta = 0$ ) or if the regularization is excessively strong ( $\beta = 10$ ). This decline in performance is particularly pronounced in the case where  $\beta = 10$ .